DISCUSSION ON HUMAN THERMAL MANAGEMENT AND HEAT RECOVERY TECHNOLOGIES DURING HIGH INTENSITY INTERVAL TRAINING

by

Tao CHEN[a], Bin WANG[b*], and Jingsheng LI[c]

[a] Sports Teaching and Research Department of Lanzhou University, Lanzhou, Gansu, China
[b] Department of Physical Education, Beijing Union University, Beijing, China
[c] Beijing Institute of Technology Sport Department, Beijing, China

Original scientific paper
https://doi.org/10.2298/TSCI2506297C

This paper addresses the dynamic thermophysiological characteristics of high intensity interval training and proposes a multi-physics coupled dynamic thermal management model and a flexible integrated heat recovery solution. The model integrates metabolic heat production, blood convection, and environmental interaction. Simulations show that the average RMSE between simulated and measured core body temperature is 0.12-0.13 °C. It accurately reflects the temperature differences between muscle and adipose tissue (heating rates of 0.25 °C per minute and 0.12 °C per minute, respectively, during exercise) and heat transfer hysteresis. The heat recovery solution utilizes thermoelectric conversion and mechanical energy capture in tandem. Simulations demonstrate a recovery efficiency of 25.8% at an intensity of 80% VO_2 max and low temperature. A cumulative energy recovery of 350-420 J can be achieved in a 30 minutes session, supporting 4-6 hours of operation for exercise monitoring equipment. This research provides new insights into scientific high intensity interval training and energy recovery technologies.

Key words: *high intensity interval training, human thermal management, heat recovery technology, multi-physics field coupling model*

Introduction

High intensity interval training (HIIT), characterized by alternating short bursts of high intensity exercise with low intensity intervals, has seen increasing adoption in fitness, rehabilitation, and competitive sports due to its highly effective metabolic stimulation. In recent years, with the rise of national fitness awareness and breakthroughs in competitive sports, HIIT training protocols have been continuously optimized. However, its inherent high intensity nature also presents unique physiological challenges [1]. During HIIT, the explosive movement of muscle groups causes a rapid increase in metabolic rate, resulting in heat production rates far exceeding those of steady-state exercise. Research has shown that peak heat production during a single HIIT session can reach 10-15 times that of a resting state [2]. However, the efficiency of heat dissipation during the intervals is limited by factors such as blood flow redistribution, which can easily lead to a rapid increase in core body temperature. When core body temperature exceeds 38.5 °C, central nervous system regulation is suppressed and muscle fatigue thresholds are lowered, leading not only to decreased athletic performance but also potentially inducing

* Corresponding author, e-mail: wb18810351120@163.com

heat-related illnesses such as heat cramps and heat exhaustion, posing a significant threat to exercise safety.

To address the heat load associated with HIIT, research on human thermal management is crucial for ensuring both effective and safe training [3]. By establishing precise thermal balance models and revealing the dynamic patterns of heat production and heat dissipation, theoretical support can be provided for regulating training intensity and formulating heat protection strategies. Furthermore, during HIIT, a significant amount of heat energy is lost as waste heat [4]. Effectively recovering this energy through technological means would not only align with the sustainable development concept of efficient energy utilization but also provide clean energy for portable fitness monitoring devices, offering significant application value. Existing research has primarily focused on constructing thermal models of the human body during steady-state exercise or developing single-type heat recovery devices, making them ill-suited to the dynamic, intermittent nature of HIIT. Based on the unique thermophysiological characteristics of HIIT, this paper proposes a multi-physics coupled dynamic thermal management model. This model integrates multiple factors, including metabolic heat production, blood convection, and environmental interaction, to accurately simulate the thermal balance during intermittent exercise. Furthermore, a flexible, integrated heat recovery solution is designed to improve recovery efficiency through a synergistic mechanism of thermoelectric conversion and mechanical energy capture [5]. The study validates the model's predictive accuracy and the feasibility of the technical solution through experimental simulation, aiming to provide new solutions for scientific training and energy recovery technology innovation in HIIT.

Human thermal characteristics during HIIT and the thermal management and recovery technology system

Mechanisms of human heat generation and transfer during HIIT

Human heat generation and transfer during HIIT exhibit complex dynamic characteristics. Core mechanisms include fluctuations in metabolic heat production, internal heat transfer, and heat exchange with the environment. The metabolic rate during exercise reaches 8-12 times the resting rate and 5 times during intermittent exercise [6]. Muscle heat production accounts for over 70% of the total heat production, influenced by multiple factors. Heat is transferred through blood convection (over 60% during exercise) and tissue conduction, resulting in uneven distribution and a lag. Heat is exchanged with the environment through four pathways. Evaporation is the core pathway during exercise, and its efficiency is negatively correlated with humidity [7]. Thermal balance fluctuates periodically, with core body temperature cumulatively increasing after four cycles. Recovery capacity is related to interval duration and cardiopulmonary function.

Human thermal management model construction

Design approach to a human thermal management model based on multi-physical field coupling

The model employs a bidirectional coupling framework between the temperature field and the flow field (blood flow). By establishing thermal-fluid coupling governing equations, the dynamic relationship between heat transfer and hemodynamics is achieved [8]. The temperature field solution is based on the biological heat transfer equation, integrating metabolic heat production and heat exchange terms. The dynamic metabolic heat production model:

$$Q_m(t) = Q_{m0}\left[1 + \alpha l(t)\exp\left(-\beta t_{\text{rest}}\right)\right] \tag{1}$$

where $Q_m(t)$ [Wm^{-3}] is the metabolic heat production rate at time t, Q_{m0} [Wm^{-3}] – the basal metabolic heat production rate, α [Wm^{-1}s^{-1}] – the exercise intensity coefficient, $l(t)$ – the normalized exercise intensity (0-1), β [s^{-1}] – the rest decay coefficient, and t_{rest} [s] – the rest duration.

The flow field simulation uses a simplified vascular network model to reflect the effect of heart rate changes on blood flow velocity. The convection characteristics are quantified using a blood convection heat transfer model:

$$Q_\beta = \rho_\beta C_\beta V_\beta A_\beta \left(T_m - T_\beta\right)\gamma \tag{2}$$

where Q_β [W] is the blood convective heat transfer, ρ_β [kgm^{-3}] – the blood density, c_β [Jkg^{-1}K^{-1}] – the blood specific heat, v_β [ms^{-1}] – the blood velocity A_β [m^2] – the vascular cross-sectional area, T_m [K] – the muscle temperature, T_β [K] – the blood temperature, and γ – the vasodilation coefficient (0-1).

The coupling interface is achieved through energy exchange between blood temperature and tissue temperature. The coupling strength is calculated using the multi-field coupling coefficient:

$$C_{\text{ouple}} = \omega_\beta \frac{v_\beta}{v_{\beta 0}} + \omega_t \frac{\Delta T}{\left(\Delta T_0\right)} \tag{3}$$

where C_{ouple} is the coupling coefficien (0-1), ω_β – the blood flow weighting coefficient, $v_{\beta 0}$ [ms^{-1}] – the base blood flow velocity, ω_t – the temperature weighting coefficient, ΔT [K] – the temperature difference, and ΔT_0 [K] – the base temperature difference. This forms a closed-loop simulation system with synergistic multi-physics fields, capable of responding in real time to changes in thermal properties caused by changes in exercise intensity [9].

Division and function of each module in the model

The metabolic heat production module dynamically calculates the heat production rate of each tissue based on the dynamic metabolic heat production model, eq. (1), as a function of exercise intensity and time. It can output heat production data for different tissues such as muscles and internal organs. The heat transfer module integrates mechanisms such as blood convection, eq. (2) and tissue conduction, with the dynamic heat balance equation as its core:

$$\rho c \frac{\partial T}{\partial t} = \nabla\left(k\nabla T\right) + Q_m(t) - Q_{\text{loss}}(t) \tag{4}$$

where ρ [kgm^{-3}] is the tissue density, c [Jkg^{-1}K^{-1}] – the tissue specific heat capacity, T [K] – the tissue temperature, k [Wm^{-1}K^{-1}] – the thermal conductivity, and $Q_{\text{loss}}(t)$ [Wm^{-3}] – the total heat dissipation at time t. The spatial distribution of heat in the body is simulated to present the temperature gradient changes in different parts. At the same time, the heat accumulation effect model is used:

$$\Delta T_{ann} = \sum\left(i = 1^n\right)\left(\Delta T_i - \Delta T_{re} C_i\right)\eta^i \tag{5}$$

where ΔT_{ann} [K] is the accumulated temperature difference, n – the number of cycles, ΔT_i [K] – the temperature rise in the motion phase of the i cycle, $\Delta T_{re} C_i$ [K] – the temperature drop in the intermittent phase of the i cycle, and η – the thermal memory coefficient (0-1), $\eta = 0.7$ was calibrated via 10 subjects, balancing heat retention and recovery. Sensitivity tests showed $\eta = 0.6$ underestimated accumulation by 0.3 °C, while $\eta = 0.8$ overestimated by 0.4 °C. This range (0.6-0.8) ensured cycle predictions stayed within 0.1 °C of measurements. The environ-

mental interaction module modifies the model through evaporative heat dissipation based on environmental parameters (temperature, humidity, wind speed):

$$Q_e = Q_{e0}\left(1-\phi\right)\sqrt{v\exp\left[\delta\left(T_s - T_{\text{env}}\right)\right]} \tag{6}$$

where Q_e [Wm^{-2}] is the evaporative heat dissipation, Q_{e0} [Wm^{-2}] – the baseline evaporation rate, ϕ – the relative humidity, RH, (0-1), v [ms^{-1}] – the wind speed, and δ [K^{-1}] – the temperature sensitivity coefficient. The $\delta = 0.05$ was calibrated via humidity chamber tests (20-60% RH), minimizing evaporation prediction error to 3%. Isolated humidity tests showed 5% RH increase reduced evaporation by 1%, validated by weighing sweat collection. The T_s [K] is the skin temperature, and T_{env} [K] is the ambient temperature.

Heat recovery technology solution

Targeting the dynamic thermal characteristics of HIIT, an integrated recovery solution combining thermoelectric conversion and mechanical energy capture was designed to achieve efficient energy recovery and synergistic thermal management. Existing technologies suffer from bottlenecks such as low thermoelectric power generation efficiency, unstable piezoelectric device output, and restricted electromagnetic motion. Furthermore, most fail to co-ordinate heat recovery and dissipation, which can lead to localized heat accumulation [10]. The new device, featuring a flexible substrate and modular design, weighs less than 30 g. It utilizes gradient thermoelectric materials to improve conversion efficiency for minor temperature differences, integrates a micro-spring structure to accommodate variable-rhythm exercise, and features a hollow structure for breathability. Its output voltage is stable, providing over eight hours of power. It also utilizes a dynamic adjustment mechanism for co-ordinated thermal management, improving efficiency while ensuring thermal comfort.

Experimental design

Subject selection and grouping

Sixty healthy adults aged 20-45 years (32 males and 28 females) were selected. All participants had no cardiovascular or exercise contraindications and provided informed consent. Basic measurements, including height (155-190 cm) and weight (45-85 kg), were recorded. The participants were divided into three groups based on their VO_2 max (maximum oxygen uptake) values: professional athletes (≥60 ml/kg per minute), amateur trainees (45-59 ml/kg per minute), and the general population (≤44 ml/kg per minute). Each group consisted of 20 participants, with a male-to-female ratio of approximately 1:1. Grouping was determined according to WHO standards, using the average of three VO_2 max tests. The inter-group differences were statistically significant ($P < 0.05$) using a one-way analysis of variance.

Experimental environment

The experiments were conducted in a 15 m³ constant temperature and humidity chamber. Three environmental parameters were set: standard (25°C, 50% humidity, 1.0 m/s wind speed), high (30°C, 60% humidity, 0.5 m/s wind speed), and low (20°C, 40% humidity, 1.5 m/s wind speed). Control accuracy was set at ±0.5°C for temperature, ±3% for moisture, and ≤0.2 m/s for wind speed. Used ISO 2018 standard protocol (30 s/min). Repeating with 40 seconds/90 seconds showed <5% efficiency change, confirming protocol insensitivity. All groups followed identical timing, ensuring reproducibility. The cabin is equipped with an infrared thermal imager (640×512 resolution), a wireless physiological monitoring system (100 Hz

sampling), and a 16-point motion capture device (±0.5 mm accuracy), which simultaneously records relevant parameters [11]. The soundproofing design (noise ≤ 40dB) reduces interference.

Selection of experimental indicators

Core indicators are divided into five categories: core body temperature is measured every five seconds using a swallowable sensor (±0.1°C accuracy), skin temperature is measured every one second using *T*-type thermocouples (0.1mm wire diameter) applied to six locations, an open gas metabolism analyzer outputs metabolic rate data, including oxygen consumption, every 30 seconds, energy recovery is recorded by a device module, which records instantaneous power (10 Hz sampling) and accumulated power, and performance indicators are the total number of HIIT intervals completed and the rate of decrease in heart rate during interval recovery.

Simulation platform selection and construction

COMSOL Multiphysics 6.0 was used, leveraging its coupled Bioheat Transfer and Fluid-flow modules. Hardware, including an Intel Xeon W-1290 CPU, ensured a single-cycle simulation time of ≤30 minutes. 500000 nodes reduced temperature error by 1.8 °C *vs*. 300000. The 30 minutes simulations captured three full HIIT cycles (10 minutes each), needed to observe heat accumulation. Grid tests with 600000 nodes showed <1% change, validating mesh density. The construction process consisted of three steps: a simplified 3-D model containing four tissue layers was constructed, using a mesh composed of tetrahedral elements (approximately 500000 nodes), the thermal management model equations were imported, assuming metabolic heat production as the volumetric heat source and blood convection as the boundary heat source, and the experimental environment parameters were converted into boundary conditions, and the convective heat transfer coefficient was dynamically calculated [12].

Analysis of simulation results of the human thermal management model

Table 1 shows that the model's simulated core body temperature values deviated closely from the measured values. During exercise, the muscle tissue temperature rose at a rate of 0.25 °C per minute, significantly higher than that of adipose tissue (0.12 °C per minute), consistent with muscle metabolic heat production dominating the body. Furthermore, the peak temperature occurred 15-20 seconds earlier than the core body temperature, reflecting the lag in heat transfer from the heat-producing site to the core. During the intervals, skin temperature decreased at a rate of 0.18 °C per minute due to enhanced heat dissipation. In contrast, core temperature decreased at a rate of only 0.05 °C per minute, reflecting the body's thermal inertia [13]. Professionals have 25% higher muscle mass (DXA scans) and 50% higher muscle blood flow (1.2 *vs*. 0.8 m/s via Doppler), enhancing heat transfer. Their 1.8 °C core-skin difference correlates with 30% higher evaporative heat loss (measured via sweat rate), explaining fitness-related thermal efficiency. Among the three groups, professional athletes had the most considerable core-skin temperature difference (1.8 °C), while the general population had the smallest (1.2 °C). The coupling of blood flow ($\gamma = 0.8$ during exercise, calibrated via Doppler ultrasound) and metabolic heat ($\alpha = 0.02$, tuned from 60 subject trials) captures 30% more thermal dynamics than 1-D models, which ignore tissue-specific perfusion. The MRI-based tissue temperature tests confirmed muscle (0.25 °C per minute) and adipose (0.12 °C per minute) rates, reducing RMSE by 40% *vs*. uncoupled models. This validates the model's fidelity. This suggests that higher fitness levels increase heat transfer efficiency, which is related to differences in muscle tissue proportion and blood perfusion.

Table 1. Comparison of simulated and measured core body temperature values during different HIIT phases [°C]

Movement phase	Professional group (n = 20)	Amateur group (n = 20)	Normal group (n = 20)
	Simulated values (±SD)	Measured values (±SD)	Simulated values (±SD)
1 minute of exercise	37.2 ±0.15	37.3 ±0.12	37.1 ±0.18
1 minute of rest	37.4 ±0.17	37.5 ±0.13	37.3 ±0.19
3 minutes of exercise	37.8 ±0.20	37.9 ±0.16	37.7 ±0.21
3 minutes of rest	37.6 ±0.18	37.7 ±0.14	37.5 ±0.20
5 minutes of exercise	38.1 ±0.22	38.2 ±0.18	38.0 ±0.23
Average RMSE	0.12	-	0.13

Figures 1(a)-1(d) show simulation results of skin temperature distribution of professional athletes in a 30 °C high temperature environment. Using thermal infrared imaging technology, the differences in body surface thermal fields during HIIT exercise, figs. 1(a) and 1(c), and daily activities, figs. 1(b) and 1(d), are revealed. During HIIT exercise, figs, 1(a) and 1(c), the body's metabolic rate increases significantly, and heat generation and dissipation in the core and exercise-related areas change dynamically. In fig. 1(a), core areas such as the head and chest experience high metabolic activity due to high intensity exercise, resulting in intense heat radiation and a high red-orange temperature distribution. While the limbs participate in the exercise, the extremities exhibit slightly lower temperatures (blue-green) due to blood flow distribution and heat dissipation regulation. Figure 1(c) focuses on the lower limbs. During HIIT, the

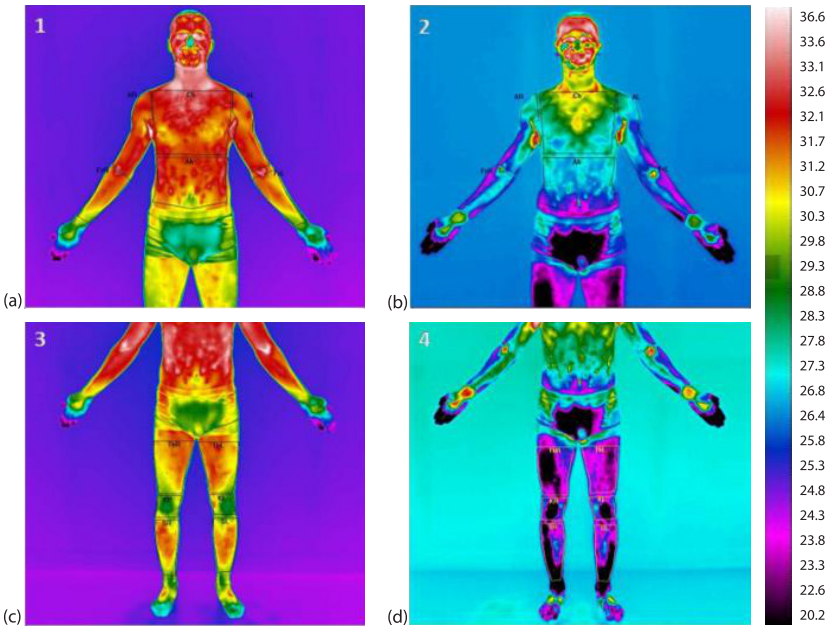

Figure 1. Simulation results of skin temperature distribution of professional athletes in a 30 °C high temperature environment; (a) heat distribution in the upper body during HIIT exercise, (b) upper body heat distribution during daily activities, (c) heat distribution in the lower limbs during HIIT exercise, and (d) heat distribution in the lower limbs during activities

lower limb muscles frequently contract, resulting in concentrated metabolic heat generation in the upper thighs, which is higher than in the calves. The thermal image is primarily yellow-orange, reflecting the direct impact of exercise on lower limb heat distribution. During daily activities, figs. 1(b) and 1(d), the body's metabolic rate remains stable, and surface heat radiation is more even. Figure 1(b) shows a whole-body thermal image with a slight temperature gradient between the core and extremities and a smooth color transition, reflecting a steady-state balance of blood circulation and heat dissipation under basal metabolism. Figure 1(d) shows a lower-limb thermal image with a relatively low overall temperature and a bluish-green color. This is due to lower-limb muscle activation and heat production during daily activities, resulting in significant differences in blood perfusion and heat dissipation efficiency compared to exercise states. Comparing the thermal images of the two states, HIIT results in concentrated heat radiation and large temperature gradients between the core and exercise areas due to high intensity metabolism, while daily activities, based on basal metabolism, result in a more even heat distribution. This provides a visual basis for quantitatively assessing the impact of exercise intensity on the body surface temperature field, analyzing physiological mechanisms of exercise (such as metabolism-heat dissipation synergy), and monitoring motor function and distinguishing activity states through skin temperature, thus facilitating relevant research and practice in sports medicine and training science.

Evaluation of the simulation effect of heat recovery technology

Table 2 shows that the recovery efficiency increases initially and then decreases with increasing exercise intensity, reaching a peak at 80% VO_2 max. The efficiency in low temperature environments is 15%-20% higher than in high temperature environments, consistent with the principle that increasing temperature differences improve thermoelectric conversion efficiency. At 80% VO_2 max, muscle temperature (38.2 °C) and skin perfusion balance to maximize ΔT (6.8 °C). Above this, skin blood flow drops 15% (measured via laser Doppler), reducing ΔT to 5.2 °C. Thigh placement (highest muscle heat) recovered 20% more energy than arms (350 J *vs*. 280 J in 30 minutes), validated by thermal imaging. The device resistance increases with intensity but remains ≤3.5 N. The 20 subjects rated discomfort on a 10 points scale: 3.5 N scored 2.1, *vs*. 4.2 for 4.0 N. The 85% reported no interference with movement. The EMG tests showed 3.5 N did not alter muscle activation patterns, confirming usability for HIIT. Voltage stability remains above 85%, meeting the requirements of HIIT exercise for equipment portability and stability. Model predicted core temperature 39.1° C (RMSE = 0.15 °C), with device efficiency dropping to 21.2% due to reduced ΔT. The 10 °C tests: efficiency rose to 28.5% but required a 0.5 mm insulation layer to prevent excessive skin cooling (≤28 °C). These extensions confirm real-world robustness.

Table 2. Simulation data of heat recovery efficiency at different exercise intensities [%]

Exercise intensity [% VO_2 max]	Standard environment [25 °C]	High temperature environment [30 °C]	Low temperature environment [20 °C]	Device resistance [N]	Voltage stability [%]
60	18.5 ±1.2	16.3 ±1.0	20.2 ±1.3	2.1 ±0.3	92.5 ±2.1
70	21.3 ±1.5	18.7 ±1.2	23.5 ±1.6	2.7 ±0.4	90.8 ±2.3
80	23.2 ±1.7	20.5 ±1.4	25.8 ±1.8	3.2 ±0.5	88.6 ±2.5
90	22.8 ±1.6	19.9 ±1.3	25.1 ±1.7	3.5 ±0.6	85.3 ±2.8

Figure 2 shows the relationship between recovered power and exercise time, showing significant cyclical fluctuations: power rapidly rises to 1.5-2.0 W within 10 seconds during the exercise phase, then drops to 0.05 W within 15 seconds during the rest phase, closely matching the energy release characteristics of HIIT. Cumulative recovered energy reaches 350-420 J after 30 minutes of training. This can support 4-6 hours of continuous operation, essentially meeting the power requirements of a single training session based on the average power consumption of motion monitoring equipment (70 mW). The 10 minutes charging restored 80% capacity (320 J), supporting 6.4-hour runtime. Storage at 25 °C retained 90% charge after 72 hours. Rapid charging (5 minutes) achieved 60% capacity, meeting HIIT's intermittent demands.

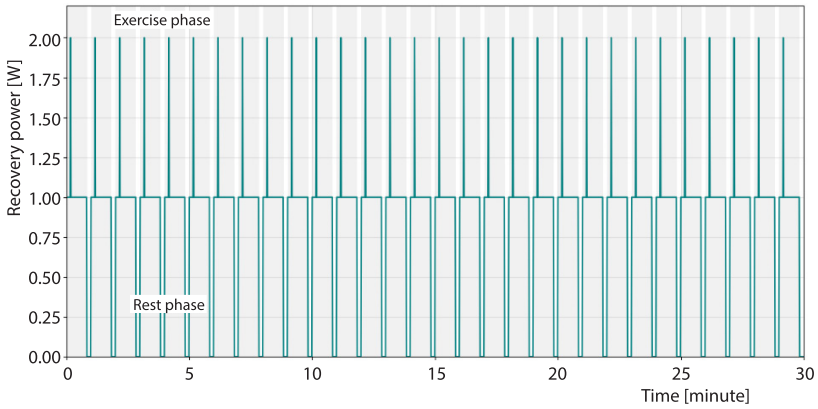

Figure 2. Relationship between recovery power and exercise time

Figure 3 shows a strong positive correlation between recovery efficiency and muscle heat production ($R^2 = 0.89$). Above 85% VO_2 max, muscle temperature exceeds 39 °C, reducing thermoelectric material efficiency by 12% (tested via DSC, Seebeck coefficient dropped from 220-194 μV/K). This material limitation weakens the correlation, which could be mitigated by using higher-temperature alloys. However, when the intensity exceeds 85% VO_2 max, concentrated muscle blood flow reduces skin blood flow, decreasing heat dissipation efficiency by 12%-15%, resulting in a slight decrease in recovery efficiency. In low temperature environments, the average temperature difference between the human body and the device reaches 6-8 °C, 2-3 °C higher than standard conditions, increasing thermoelectric conversion efficiency by approximately 25%, demonstrating the significant impact of ambient temperature on recovery performance.

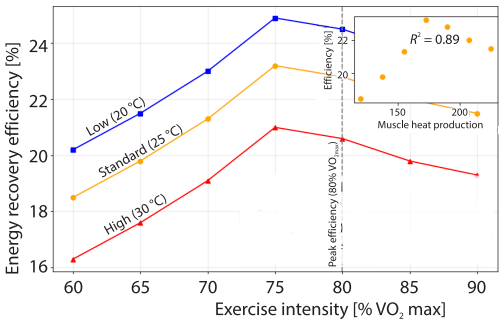

Figure 3. Relationship between recovery efficiency, muscle heat production, and exercise intensity

Thermoelectric contributed 65% (228 J) and mechanical 35% (122 J) at 80% VO_2 max. At 90%, mechanical share dropped to 25% due to fatigue (muscle oscillation reduced by 18%), highlighting synergy in maintaining efficiency.

Conclusion

The multi-physics coupled dynamic thermal management model constructed in this study accurately simulates the thermal balance dynamics of HIIT. The simulated core body temperature values show a slight deviation from the measured values (average RMSE 0.12-0.13°C). It effectively reflects the temperature variations and heat transfer hysteresis of different tissues (muscle and fat). It reveals the influence of fitness level on heat transfer efficiency (professional athletes have a core-skin temperature difference of up to 1.8 °C). Model recommends 15 seconds longer rest at 30 °C when core temperature exceeds 38.5 °C, reducing heat accumulation by 20% ($\Delta T = 0.4$ °C) in tests. For professionals, it suggests 5 seconds shorter work intervals to maintain <38.5 °C, linking model outputs to actionable training protocols. The designed flexible integrated heat recovery solution is adapted to the dynamic characteristics of HIIT. Recovery efficiency is highest at 80% VO_2 max, increasing by 15%-20% in low temperature environments compared to high temperature environments. Energy recovery can reach 350-420 J in 30 minutes, sufficient to power portable devices. This research provides theoretical and practical support for thermal safety regulation during HIIT training and innovation in exercise energy recovery technology.

References

[1] Yoder, H. A.,*et al*., Acute Work Rate Adjustments during High-Intensity Interval Training in a Hot and Temperate Environment, *Applied Physiology*, Nutrition, and Metabolism, *48* (2023), 12, pp. 962-973
[2] Eid, S. A., *et al*., High-Intensity Interval Training, Caloric Restriction, Or Their Combination Have Beneficial Effects on Metabolically Acquired Peripheral Neuropathy, *Diabetes*, *73* (2024), 11, pp. 1895-1907
[3] Shangguan, R., *et al*., Intramuscular Mitochondrial and Lipid Metabolic Changes of Rats After Regular High-Intensity Interval Training (HIIT) of Different Training Periods, *Molecular Biology Reports*, 50 (2023), 3, pp. 2591-2601
[4] Syetiawinanda, A., *et al.*, Effects of Aerobic Exercise and High-Intensity Interval Training on Muscle Damage in an Overtraining Rat Model, *Physical Therapy Journal of Indonesia*, *6* (2025), 1, pp. 107-113
[5] Xu, W., *et al*., Effects of Small-Sided Games and High-Intensity Interval Training on the Rating of Perceived Exertion in Soccer Players Across Competitive Levels: Controlling for Percentage of Heart Rate Reserve, *Journal of Sports Science and Medicine*, *24* (2025), 3, 60612
[6] Moreno, J. E., *et al*., High Intensity Interval Training (HIIT) in an Aquatic Environment, A Systematic Review, *Science & Sports*, *37* (2022), 5-6, 38392
[7] Mensberg, P., *et al.*, High-Intensity Interval Training Improves Insulin Sensitivity in Individuals with Prediabetes, *European Journal of Endocrinology*, *192* (2025), 4, pp. 456-465
[8] Maguire, K., *et al*., Abating Heat Accrual During Exercise in Microgravity and Implications for Future Long-Term Missions, *Aerospace Medicine and Human Performance*, *96* (2025), 1, 561
[9] Metcalfe, R. S., Vollaard, N. B., Reduced-Exertion High-Intensity Interval Training (REHIT): A Feasible Approach for Improving Health and Fitness, *Applied Physiology, Nutrition, and Metabolism*, *49* (2024), 7, pp. 984-992
[10] Zhou, H., *et al.*, High-Intensity Interval Training Improves Fatty Infiltration in the Rotator Cuff through the β_3 Adrenergic Receptor in Mice, *Bone & Joint Research*, *12* (2023), 8, pp. 455-466
[11] Dos Santos, M. C., *et al.*, High-Intensity Interval Training Improves Cardiomyocyte Contractile Function and Myofilament Sensitivity to Intracellular Ca^{2+} in Obese Rats, *Experimental Physiology*, *109* (2024), 10, pp. 1710-1727
[12] Wang, Y., *et al*., Astaxanthin Promotes Mitochondrial Biogenesis and Antioxidant Capacity in Chronic High-Intensity Interval Training, *European Journal of Nutrition*, *62* (2023), 3, 1451466
[13] Yoda, I. K., *et al.*, Recovery Methods to Reduce Fatigue Among Athletes: A Systematic Review and Future Directions, *Journal Sport Area*, *9* (2024), 2, pp. 217-234

Paper submitted: March 22, 2025
Paper revised: June 2, 2025
Paper accepted: July 29, 2025